Heliyon 9 (2023) e13554

Contents lists available at ScienceDirect

Heliyon

journal homepage: www.cell.com/heliyon

Research article

Heparin-based sericin hydrogel–encapsulated basic fibroblast growth factor for in vitro and in vivo skin repair

Pan Du [a], Ling Diao [b], Yichi Lu [a], Chenyang Liu [b], Jin Li [a], Yang Chen [c], Junfeng Chen [a], Guozhong Lv [a,b,**], Xue Chen [a,*]

[a] Wuxi Medical School, Jiangnan University, Wuxi, 214122, China
[b] The Affifiliated Hospital of Jiangnan University, Jiangsu, 214000, China
[c] Nanjing University of Chinese Medicine, Nanjing, 210000, China

ARTICLE INFO

Keywords:
Sericin hydrogel
bFGF
Wound healin

ABSTRACT

The treatment of full-thickness cutaneous wounds remains a significant challenge in clinical therapeutics. Exogenous growth factor (GF) has been applied in clinics to promote wound healing. However, the retention of GF on the wound bed after its direct application to the wound surface is difficult. Moreover, growth factors (GFs) are always inactivated in the complex wound healing microenvironment due to various factors, which significantly decrease the therapeutic effect. Sericin hydrogel (S) can be used as an effective carrier for GFs owing to its low immunogenicity, good biocompatibility, and good healing-promoting ability. Here, we designed a heparin-based sericin hydrogel (HS) -encapsulated basic fibroblast growth factor (bFGF-HS) to facilitate wound healing and skin regeneration. The hydrogel exhibited a three-dimensional (3D) microporous structure, excellent biodegradability, good adhesiveness, and low cytotoxicity. In vitro release of bFGF from bFGF-HS coacervates revealed that bFGF-HS might control the release of bFGF within 25 days through heparin regulation. bFGF-HS significantly promoted vascularization and re-epithelialization and improved collagen deposition, ultimately accelerating wound healing in vivo in mice. bFGF-HS treated wounds were also found to have more hair follicles and milder inflammatory reactions. Overall, this study provides a new therapeutic approach for full-thickness skin defect wounds using bFGF-HS.

1. Introduction

The skin is the body's first line of defense against harmful elements in the external environment [1,2]. Various external or internal factors can cause wounds such as burns, sharp injuries, radiation damage, pressure ulcers, and diabetic ulcers. Administering inadequate treatment leads to incomplete skin regeneration, wound scarring, and delayed healing [3–6]. Generally, wound healing is a dynamic, orderly, and complex process that includes four overlapping processes: hemostasis, inflammation, proliferation, and remodeling [7–10]. Numerous strategies are available for wound healing; among them, dressings have been demonstrated to promote wound healing. Currently, several wound dressings are used clinically, including hemostatic sponges, bacterial cellulose, foams, nanoparticle materials, and hydrogels [11–15]. A humid environment has been demonstrated to provide a suitable environment for the

* Corresponding author.
** Corresponding author. Wuxi Medical School, Jiangnan University, Wuxi, 214122, China.
E-mail addresses: luguozhong@hotmail.com (G. Lv), snow@jiangnan.edu.cn (X. Chen).

https://doi.org/10.1016/j.heliyon.2023.e13554
Received 13 December 2022; Received in revised form 3 February 2023; Accepted 3 February 2023
Available online 9 February 2023

proliferation of wound cells. Such environment can accelerate the migration of epidermal cells and enhance the secretion of cells, thereby effectively promoting wound healing [16,17]. The water content of hydrogel dressings is very high; this may result in the wound surface being moist and sterile, in line with the wet wound healing theory. Numerous studies have shown that hydrogels can effectively accelerate wound healing by promoting cell proliferation, quick hemostasis, and the absorption of secretions in wounds [18]. Sericin can also be loaded with various drugs or active factors to more effectively accelerate wound healing [19,20].

Sericin is secreted by the silkworm's central silk gland and is one of the two main proteins that constitute the cocoon, accounting for approximately 20–30% of the cocoon content [21]. Sericin is a waste by-product of the textile industry that is often dumped in wastewater used for degumming, thereby having an environmental impact as a water pollutant [22]. Sericin is a natural macromolecular viscous protein that is wrapped on the surface of silk fibroin fibers. In recent years, several studies have been conducted using sericin owing to its extraordinary qualities, such as biocompatibility, biodegradability, oxygen and water vapor permeability, and low allergenicity and immunogenicity [23–25]. In particular, sericin as a wound dressing has been found to accelerate wound healing in many studies [26].

Cellular interactions between several cell types, including fibroblasts, keratinocytes, endothelial cells, neutrophils, and macrophages, are necessary for wound healing. These interactions are mediated at the wound site by endogenously released growth factors (GFs), cytokines, and chemokines [27–29]. GFs promote tissue regeneration by regulating cell proliferation and differentiation. Fibroblast growth factor (bFGF) is a crucial growth factor [30]. However, endogenous bFGF is sometimes insufficient for wound healing. Therefore, supplementation with exogenous bFGF is important to accelerate wound healing. Studies have shown that exogenous bFGF can be used in the clinical treatment of wounds and has achieved promising results. However, because to its quick in vivo turnover and short serum half-lives, exogenous bFGF may have a drastically reduced therapeutic impact [31]. Owing to the controllable degradability and high porosity of hydrogels, these materials are popular drug carriers that can encapsulate and sustainably release bFGF [32]. However, owing to their high water content, GFs tend to quickly diffuse out of the hydrogels as no moieties are available for them to attach.

Heparin is a glycosaminoglycan that is commonly used as an anticoagulant. According to Johnson and Wang's studies, a bioactive heparin-based coacervate produced quick and thorough wound healing via regulated distribution of heparin-binding EGF-like GFs, and they eventually proved its long-term efficacy [33]. The binding of GFs to heparin can protect their biological activity and prolong their half-life by preventing their degradation by proteases. Additionally, free heparin has the ability to reactivate cell surface low-affinity receptors, thereby promoting growth factor-cell interactions [34]. Heparin has a potent anticoagulant action that can improve local blood clotting and prevent microcirculation thrombosis [35]. Notably, according to recent research, ultrasonography does not destroy the structure or function of heparin [36].

In this study, we prepared a heparin-based sericin hydrogel (HS) precursor solution via ultrasound and added bFGF to the gel precursor solution consisting of heparin and sericin before gelation. The external morphology and porosity of the HS were observed by scanning electron microscopy. According to the results of the bFGF-HS in vitro release test, the hydrogel network is able to continuously release bFGF under the regulation of heparin. Further, comparing bFGF-HS to a negative control, HS hydrogel dressing and bFGF, animal experiments revealed that it can speed wound closure, decrease inflammation, and enhance vascularization. These results suggest that HS–encapsulated bFGF has remarkable potential for wound healing in tissue regeneration engineering.

2. Materials and methods

2.1. Preparation of the bFGF-HS delivery system

Natural mutant silk cocoons lacking fibroin were used to extract sericin (Bombyx mori, 185 Nd-s. Mw 60 ~> 250 kDa), which obtained from the Sericultural Research Institute, China Academy of Agriculture Science (Zhenjiang, Jiangsu, China). First, 1 g cocoons were cut into small pieces and then solubilized in 6 M (50 mL) lithium bromide (Aladdin, China) solution for 24 h at 35 °C. The dissolved sericin aqueous solutions were then added 10 mL Tris-HCL buffer (1 M, pH 9.0), and dialyzed by cellulose dialysis membranes (MWCO 3500 Da, Spectrum Laboratory, Inc., USA) against deionized water at room temperature for 3 days. Centrifugation (9000×*g*, 20 min, room temperature) was used to remove the insoluble residues from the dialysis membranes. The supernatant was then further concentrated by dialysis against a 10% (w/v) polyethylene glycol (PEG-6000, MW) solution to a 2% (w/v) concentration.

To form the HS gel, first, prepare 100 mg/mL heparin solution, then the 2% (wt/vol) sericin standard solutions were putted to EP tubes or molds of different shapes. Finally, 100 μL heparin solution (Aladdin, China) was immediately added to the sericin aqueous solutions and sonicated for 20 s at 30% amplitude. The mixture was left at 20 °C for 10 min to form an HS gel.

To prepare the bFGF-HS gel dressing, 500 ng/mL basic fibroblast growth factor (PeproTech, USA) was immediately added to the sericin/heparin precursor solution after sonication. After mixing, the mixed solution was placed at 20 °C for 20 min for bFGF-HS gel formation.

2.2. Scanning electron microscope (SEM)

The HS were rapidly frozen at −80 °C for 10 h and lyophilized in a vacuum freeze dryer for 48 h. Before specimens preparation, freezed the lyophilized sample with liquid nitrogen and break it vertically to obtain the cross section of the sample. The specimens were sputter-coated with gold, and the surface of the solid was observed using scanning electron microscopy (SEM; TM-3030; Hitachi, Yokohama, Japan).

2.3. Swelling ratio

There were prepared many HS that had the same size and mass. The dried gel's mass after lyophilization was calculated as Wd. The incubation of every dried gel in PBS buffer (pH 7.4, 11.0, 4.0). The filter paper was used to sufficiently absorb the surface water after periodically removing the gel blocks. WS was the mass's designation. The hydrogels were then placed in the buffer for continued swelling. When the mass of the hydrogels stay the same, the swelling ratio (SR) was calculated using Eq. (1)

$$SR(\%) = \frac{Ws - Wd}{Wd} \times 100\% \quad (1)$$

2.4. Degradation properties of the HS

1) The prepared HS was cut into pieces and weighed separately in a 24-aperture plank. 2) Three of the samples were dried and weighed to obtain the dry wet ratio of the samples. The dry weight (W1) of all samples in 1) was calculated from the dry wet ratio of samples in 2). Hydrogels were incubated in 1 mL of PBS (pH 7.4, 11.0, 4.0) at 37 °C; PBS was replaced daily. The samples were removed at different time points, dried, and weighed (W2). The sampling for each time point was repeated three times. The hydrogel degradation rate (DR) was calculated as follows: W2/W1 × 100%.

2.5. Mechanical properties of S and HS

First, The hydrogels were shaped into cuboid structures (length: 10 mm; width: 8 mm; height: 6 mm) for testing. Then, the compressive properties of the S and HS were analyzed by a mechanical testing machine (SFMIT, China) equipped with a 1000 N load cell and the speed of the compression rate was 2 mm/min. The mechanical property data was presented as mean ± SD (n = 5).

2.6. In vitro release of bFGF

The bFGF-HS and bFGF-S solutions were prepared at a concentration of 500 ng/mL (500 ng bFGF/1 mL hydrogel) and added (400 μL) to a 48-well plate (n = 3). Thereafter, 1 mL PBS was added to each well, and the plates were placed in a 37 °C incubator. At predetermined time points (1, 2, 4, 7, 14, 25, and 28 days), bFGF was collected by removing the supernatant and replacing it with an equal volume of PBS. Thereafter, the concentration of bFGF was measured by enzyme-linked immunosorbent assay (ELISA). The bFGF release experiment was carried out at 37 °C [37,38]; this is because the temperature of animals used in subsequent experiments was 37 °C. The amount of bFGF released was calculated using the initial and final concentrations: percentage of bFGF released (%) = final concentration/initial concentration × 100% (n = 4).

2.7. CCK-8 assay

To examine the cell proliferation of co-culture with human keratinocytes and dermal fibroblasts on bFGF-HS on days 3, 5, and 7, the Cell Counting Kit-8 (Beyotime, Shanghai, China) was employed. First, hydrogels were seeded at 96 wells which were covered with 2×10^3 cells. After incubation at a humidified 5% CO_2 incubator (37 °C) at different durations (1, 3 and 5 days) for different days, CCK-8 solution (10 μL per well of 96 well plate) was added to each well and incubated the plates at 37 °C for 2 h. Thereafter, Finally, a fresh 96-well plate was then filled with an equal amount of supernatant from each well, and then the absorbance at 450 nm was measured with a microplate reader (Epoch, BioTek, USA). Six wells were used for each sample.

2.8. Long-term growth of human dermal fibroblasts (HDFs) and keratinocytes inside bFGF-HS gels

For the co-culture model, HDFs (1×10^4/hydrogel) were planted, followed by a 24-h incubation period. In order to generate a bi-layered structure in vitro, human keratinocytes (HaCaT) (1×10^4/hydrogel) were then put on top with an air-liquid interface. Cells were pre-stained with distinct colors, red for HDFs and green for HaCaT, using cell tracker red CM-Dil (YEASEN) and green CFDA SE (YEASEN), respectively. After five days of co-culture, the cellular dispersion and 3D perspective inside the hydrogels were analyzed by a confocal microscope (Leica TCS SP5).

2.9. In vivo wound healing

Male BALB/c mice aged 7 weeks (SLAC, Shanghai, China) were housed in a conventional environment with a controlled temperature and humidity (25 ± 1 °C, 5%), as well as a light/dark cycle (12/12 h). Before operation, The mice were anaesthetized with pentobarbital sodium (Nanjing AIBI Bio-Technology Co Ltd, China). The hair from the dorsal area was removed with an electric razor and residual hair was removed using a depilatory cream (Veet, French). Surgical scissors and tweezers were used to excise the backs of mice to prepare a full-thickness circular skin wound of 6 mm diameter. Four groups (n = 5) of injured mice were randomly assigned and treated as follows: (1) blank (treated with saline), (2) HS (heparin-based sericin hydrogel), (3) bFGF (bFGF solution only, 100 ng/50 μL); and (4) bFGF-HS (heparin-based sericin hydrogel loaded with b-FGF). Hydrogel sheets were prepared with a diameter of 6 mm and a thickness of 1 mm. After treatment, all wounds of mice were covered with a strong adhesive 3 M membrane (Youlian, China) to

prevent wound contraction and then covered with an adhesive bandage (Hons, China). At days 0, 3, 7, and 14 after treatment, the wounds were photographed and imported into ImageJ (v1.8.0) software. Wound closure was calculated as follows: wound closure (%) = [A (0) − A (3,7,14)/A (0)] × 100%, where A (0) and A (3,7,14) represent the exposed wound area on postoperative days 0, 3, 7, and 14, respectively. All in vivo experiments were approved by the Jiangnan University Institutional Animal Ethical Committee and performed in accordance with the laboratory animal guidelines. The ethical review number is JN.No20220330c0480901 [105].

2.10. Histological analysis

On day 7 and day 14, respectively, full-thickness skin tissue from the back wound was excised with surgical scissors and forceps under anesthesia, and promptly fixed for at least 24 h at room temperature in a 4% paraformaldehyde solution. After graded dehydration with different concentrations of ethanol, samples were embedded in paraffin to prepare tissue sections, and then sliced into 4-μm-thick sections with a cryostat (RM2235; Leica CM1860/CM1860UV, Germany). After deparaffinization and rehydration, skin tissues were stained with hematoxylin and eosin (H&E; SENBEIJIA BIOTECHNOLOGY CO. Nanjing, China) for morphological evaluation. Masson's trichrome (Solarbio, China) revealed the Hair follicle regeneration and collagen dispersion at the wound site, according to the manufacturer's protocols [39,40]. A computerized slice scanner (Pannoramic MIDI, China) was used to see and image the stained parts.

2.11. Immunofluorescence analysis

The tissue sections were deparaffinized with dimethylbenzene, rehydrated for 5 min, boiled in citrate buffer water bath at 100 °C for 30 min, washed with TPBS. After that, treated with blocking buffer (Beyotime) for 1 h before overnight incubation with primary antibodies at 4 °C. The slices were incubated with the secondary antibodies for 1 h at room temperature the next day after being rinsed with TPBS. Staining with 4′,6-diamidino-phenylindole (DAPI, Adamas life, china) was done on the nuclei. The expression of the M1 macrophage marker CD86 (Abcam, USA) and the M2 macrophage marker CD163 (Abcam, USA) were used to assess the inflammatory response at the wound site [41,42]. By counting the blood vessels generated by CD31 (Abcam, USA) and a-SMA (Abcam, USA) positive cells, vascularization was assessed [43,44]. The proliferation of skin keratinocytes was evaluated by cytokeratin 14-positive cells (Abcam, USA) and antibodies against proliferating cell nuclear antigen (PCNA , Abcam, USA) [45]. Images were captured using an ortho-fluorescence microscope (Axio Imager Z2, Germany).

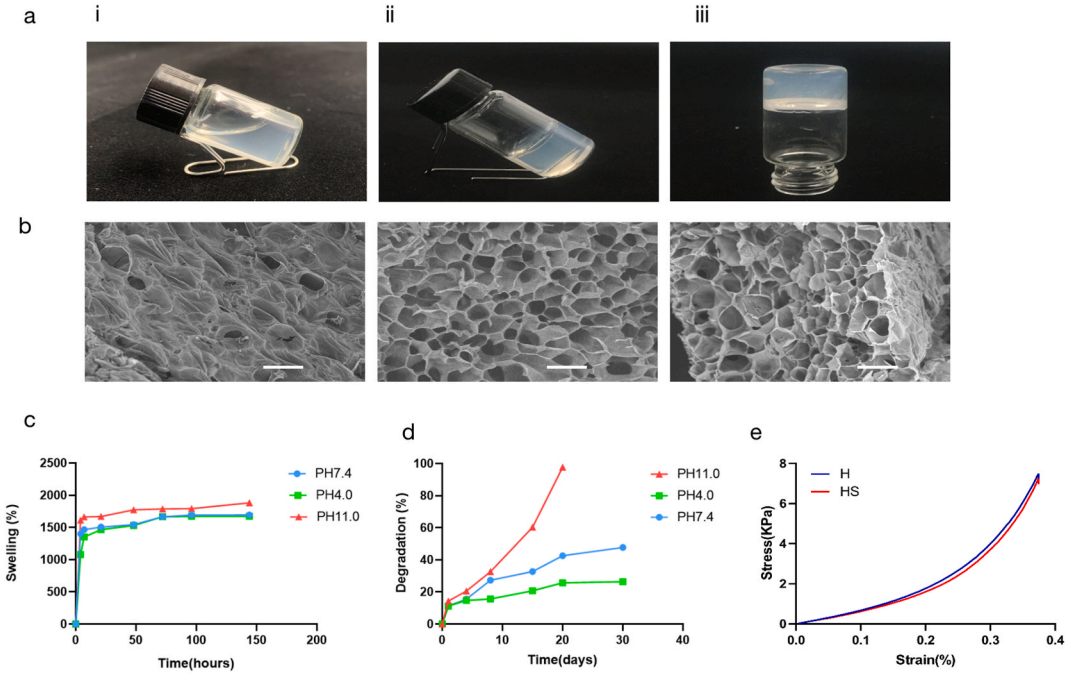

Fig. 1. Characterization of the heparin-based sericin hydrogel. Biocompatibility and sustained release of the hydrogel. (a) Inverted vial method: after gelation. (b) The surface, cross-sectional, and skewed cross-section micromorphology of the heparin-based sericin hydrogel. Scale bars, 200 mm. (c) Swelling ratio of the heparin-based sericin hydrogel in PBS (pH 7.4, 4.0, 11.0) at 37 °C. (d) In vitro degradation profiles of heparin-based Sericin hydrogel in PBS (pH 7.4, 4.0, 11.0) at 37 °C. (e) Mechanical properties test of sericin hydrogel and HS hydrogel (length: 10 mm; width: 8 mm; height: 6 mm). Data are shown as mean ± SD (n = 5 for each analysis).

2.12. Statistical analysis

All experiments were performed in triplicate, and all data are expressed as mean ± standard deviation (SD). Statistical significance was determined using one-way ANOVA. Differences were considered significant at $P < 0.05$, $P < 0.01$ and $P < 0.001$, and are indicated by * , **and ***, respectively.

3. Results

3.1. Preparation and characterization of the hydrogel

The gelation process was seen and roughly timed using the pour bottle method, as illustrated in Fig. 1a [46]. At 20 °C, the solution formed a gel within approximately 10 min. When the sample bottle was tilted, the gel solution did not flow, indicating successful gelation. The gelation period of 10 min enabled sufficient operation time for loading the GFs. In this study, The components responsible for the gelation of sonicated sericin are unknown but most likely gelation was due to ultrasonic waves enabling collisions between sericin molecules dissolved in water, by changing the protein chains' hydrophobic hydration, this mechanism may result in the formation of physical b-sheet cross-links [47], thereby produces highly stable covalent bonds to form a water-insoluble stable gel network structure. Another explanation for this gelation mode is that ultrasonic vibrations cause the development of physical cross-linkers in the gel network, which accelerates the transition of a protein from solution to gelation [48]. Ultrasonic crosslinking not only provided time control before gelation, but also did not require bio-toxic crosslinking reagents, thereby improving hydrogel biocompatibility and permitting the direct embedding of living cells.

The surface, cross-sectional, and skew cross-section micromorphology of heparin-based sericin hydrogel was investigated using SEM, as shown in Fig. 1b. As indicated by their morphological appearance, the produced hydrogels consisted of an interconnected porous network, similar to a honeycomb-like structure. The 3D network structure could allow bFGF to be loaded into and released from the HS, and support cell seeding and growth in the regeneration and healing process for wounds. Further, the 3D network structure should be conducive to nutrient exchange and metabolism between cells. The internal environment could effectively promote the healing of skin wounds.

After HS had soaked in PBS (pH 7.4, 4.0, and 11.0) for various time, the water absorption ratio was assessed. In the three pH environments, the swelling ratios of the hydrogels were very similar. In fact, the swelling ratio was approximately 1700% within 48 h (Fig. 1c). This indicates that HS has strong water absorption performance, which may be attributed to the high porosity and hydrophilicity of the hydrogels. The strong water absorption performance indicates that the extravasate can be effectively absorbed from the

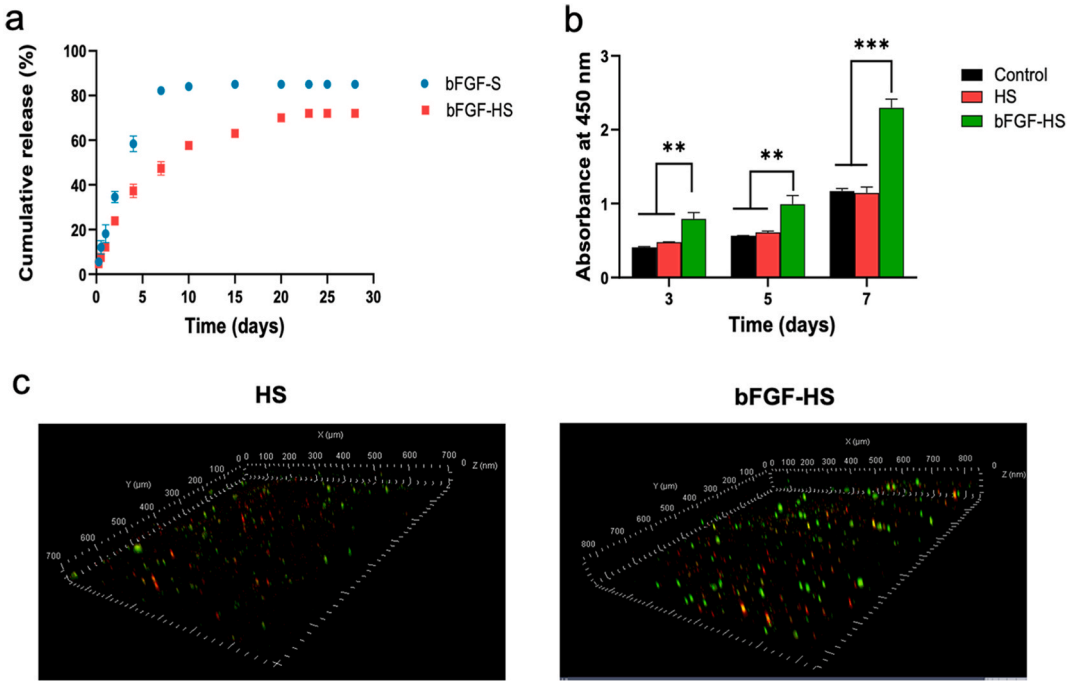

Fig. 2. Biocompatibility and sustained release of the hydrogel. (a) In vitro bFGF release profiles. (b) Determination of cellular proliferation by the CCK8 assay in growth factor (GF)-loaded HS hydrogel post co-culture with human keratinocytes and dermal fibroblasts. (c) Confocal microscopic observation of the cellular 3D distribution of pre-stained HaCaT (green) and HDFs (red) in bFGF-HS hydrogels after three, five, and seven days of co-culture. (For interpretation of the references to color in this figure legend, the reader is referred to the Web version of this article.)

wound tissue while guaranteeing wound water content to offer a good microenvironment for GF release and skin tissue growth.

After soaking in PBS (pH 7.4, 4.0, and 11.0) solution, the degradation ratio of HS was assessed at various time intervals, which was based on the weight loss of the hydrogels due to degradation. As shown in Fig. 1d, the degradation of HS in an alkaline solution (pH 11.0) was rapid, and the hydrogels were degraded entirely within 20 days. Correspondingly, at pH 4.0 and pH 7.4, the degradation of HS was markedly longer than that in the alkaline environment, and HS only degraded approximately 40% within 30 days. These results suggest that gradual degradation of HS can provide a growth space for new tissues. In addition, reoperation can be avoided to remove material from the body.

The mechanical strength of wound dressing is one of the determinative paramete for quality of healing. According to the stress-strain curves, the sericin hydrogel's mechanical properties were similar to those of HS (Fig. 1e). They have same compression at break and compressive strength. The addition of heparin did not affect the mechanical properties of sericin hydrogels. Both S and SH have good mechanical strength and flexibility. This property enables the dressing to be well applied to wounds.

3.2. Controlled release of bFGF from the bFGF-HS hydrogels

Owing to the short half-life of GFs in vivo, bFGF supplementation after direct administration is unstable and rapidly degrades after diffusion from the wound site. The therapeutic benefits of exogenous bFGF are greatly reduced by this drawback. However, using hydrogel-loaded GFs can control their release and reduce the loss of GFs in the tissue regeneration process. The release profile of bFGF from heparin-based and sericin hydrogel is depicted in Fig. 2a. Both kinds of hydrogels were shown to have an initial burst of release, allowing the patient to get a higher dosage during the initial period of therapy. For the sericin hydrogel, complete release was observed

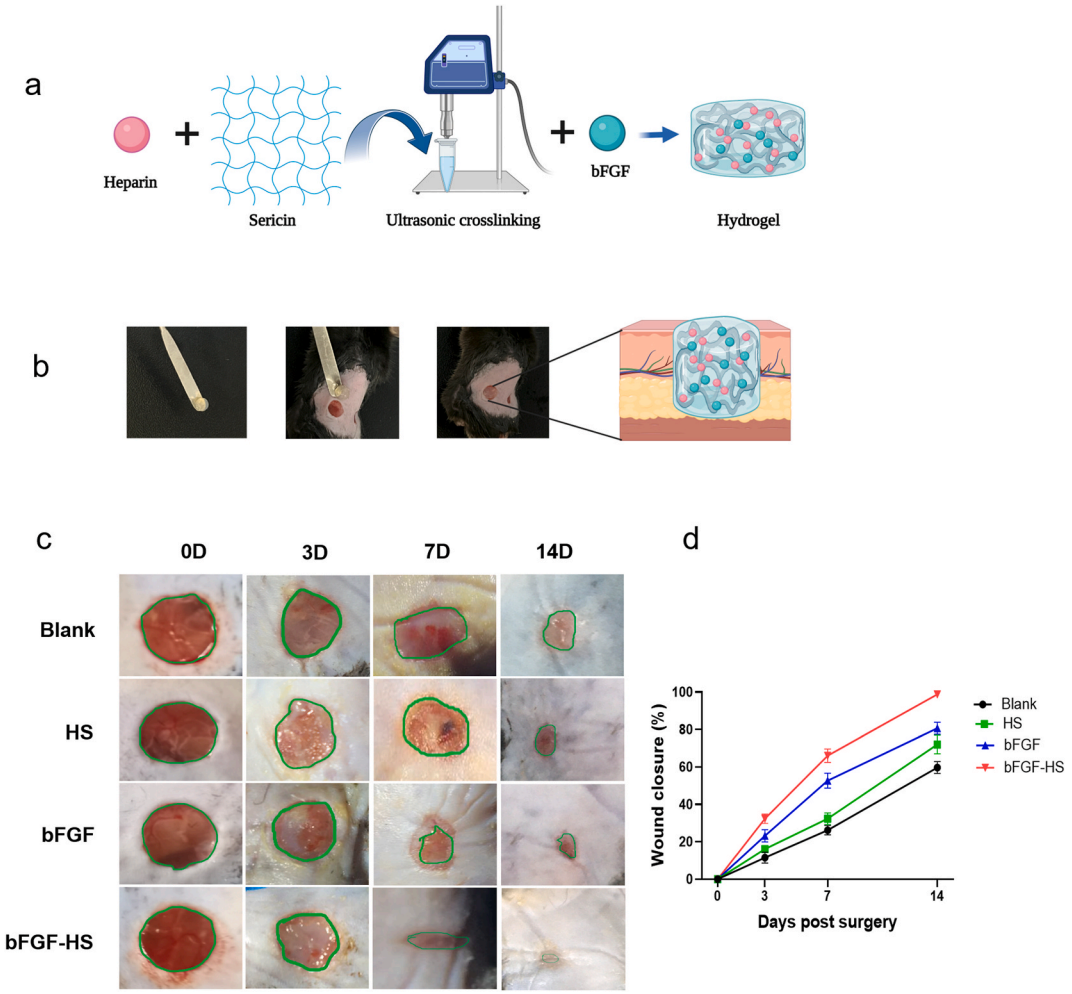

Fig. 3. Mouse wound repair process. (a) Schematic of hydrogel network loading with drug. (b) Experimental scheme for the preparation of bFGF loaded hydrogel sheet and wound healing treatment for full thickness wound. Created with BioRender.com. (c) Representative photographs of the wounds on days 0, 3, 7, and 14, dressed using saline (control), HS hydrogel, bFGF, and bFGF-HS hydrogel. (d) Wound closure over time in the wound healing model. Data are expressed as mean ± SD (n = 5).

after 7 days, with no release observed on the next day. Compared with sericin hydrogel, HS released less than 50% of the loaded bFGF in 7 days, followed by a continuous slow release over 25 days. Heparin-based hydrogels could stabilize a slightly higher amount of GFs, enabling a slow, sustained, and prolonged release. HS–encapsulated bFGF as a typical GFs delivery system, heparin can stabilize bFGF and retain its bioactivity, therefore the bFGF-HS can sustainably release encapsulated bFGF at the wound site within a few days. Thus, the HS–encapsulated bFGF dressing could be used for long-term wound healing without frequent alterations of the drug. This benefit can significantly lessen the misery of patients and reduce their financial burden.

3.3. Biocompatibility of hydrogel dressings

Human keratinocytes and fibroblasts are two of the most common cells in the connective tissues of the skin and are crucial for skin restoration. Hydrogel dressings are in direct contact with wound tissue. Thus, before the animal experiment, the hydrogel dressing was subjected to in vitro cell culture, and its ability to accelerate wound healing was initially evaluated.

Three experimental groups, each with a different dressing, Control, heparin-based sericin (HS), and bFGF-HS were established to examine the effects of each dressing component on cell growth. Based on the data from the CCK8 assay for days 3, 5, and 7, HS, and bFGF-HS were found to support the initial attachment and proliferation of fibroblasts and human keratinocytes (Fig. 2b). At each time point, the bFGF-HS group had a much higher number of live cells than the other two groups. In contrast, in the other two groups, the number of live cells was comparable at each time point. These findings suggest that bFGF is crucial for the development and proliferation of human keratinocytes and fibroblasts in hydrogel dressings.

Using a confocal microscope, after seven days of co-culture, the cell-laden hydrogels were analyzed to track how the cells had grown and migrated. Pre-stained cells that indicated fibroblasts in the bottom layer (red) and keratinocytes in the top layer (green) were used to assess how the cells were distributed in the hydrogels. As shown in Fig. 2c, compared to HS, bFGF-HS better supported the growth of the double-layered construct cells and had a deeper migration and a higher number of cells in the hydrogels. This finding indicates that the cytocompatibility of the bFGF-HS was enhanced by bFGF loading.

3.4. In vivo wound healing

To determine whether bFGF-HS can improve wound healing, we used saline, HS, and free bFGF as controls. The prepared hydrogel dressing was applied to full-thickness skin defects in mice (Fig. 3a and b). To track how the size of the wound changes over time, the wound area was photographed on days 0, 3, 7, and 14, and the wound healing rate was calculated according to the formula presented in materials and methods (Fig. 3c and d). Based on the results, on day 3 after treatment, although the wound area treated with the bFGF-HS gel had the most obvious decrease of the three groups, there was no statistically significant difference in wound healing rate among the three groups. However, after 7 days, the wound healing rate owing to the bFGF-HS gel was 67 ± 8%. The wound healing rate of the bFGF group was 51 ± 6%, while the wound healing rates of the control group and blank gel group were 22 ± 5% and 30 ± 7%, respectively. Intuitively, the bFGF-HS dressings markedly increased wound closure on day 7 compared with the other dressings. On day 14 after the operation, the wound treated with the HS containing bFGF almost completely healed, and the wound healing rate

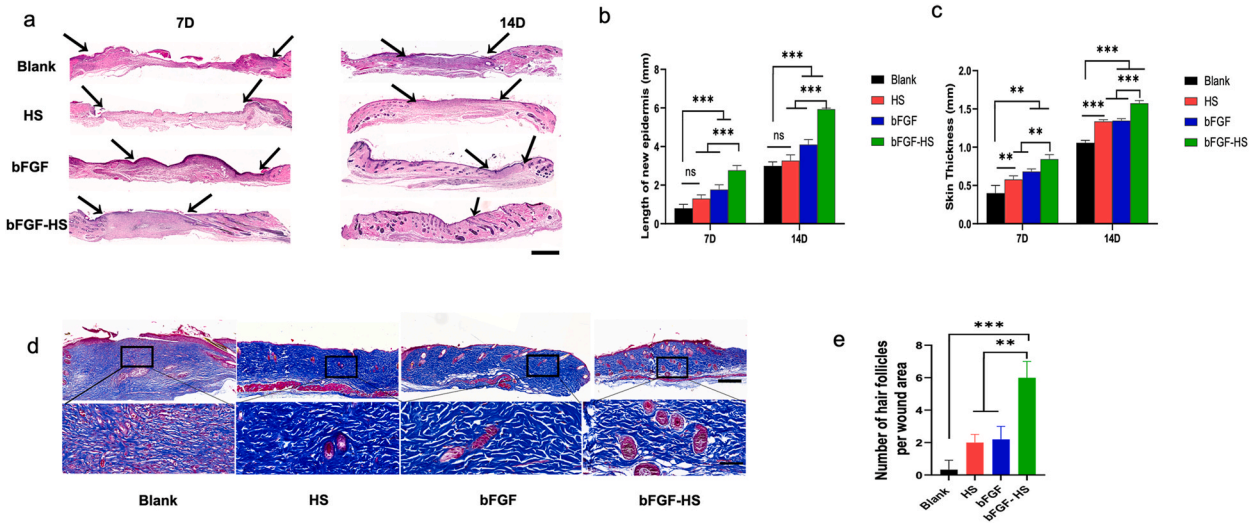

Fig. 4. Pathological examination of wound tissue. Proliferation of skin keratinocytes at wound sites in the different groups at 14 days post-surgery. (a) Hematoxylin and eosin (H&E) images of wounds treated with the different treatment materials for 7 and 14 days. Scale bars = 1 mm. Arrow indicates the epithelial junction. (b) The length of new epidermis at days 7 and 14 post-implantation. (c) Skin thickness at days 7 and 14 post-implantation. (d) Masson's staining images of wound tissues on day 14 post-surgery. Scale bar = 1 mm. (e) Number of hair follicles in the wound area. Scale bar = 200 um.

was a lot greater than the blank control group's rate (58 ± 4%), HS group (69 ± 7%), and bFGF group (81 ± 10%). Further, no obvious scar was found in the bFGF-HS group. It can be seen that among the four treatment methods, the bFGF-HS group has the best healing effect, Our results confirmed the synergistic effects of bFGF and HS.

3.5. Histological observation

In trauma therapy, the process of healing a wound involves multiple overlapping stages, including inflammatory reactions, granulation, and epithelial formation, with a series of complex and orderly biological processes [49–51]. To compare the degree of wound healing among the four groups, H&E staining was performed on mouse skin tissue in all treatment groups on days 7 and 14 after wounding. As shown in Fig. 4a–c, on day 7 post-operation, the dermis's imperfect structure in the blank group, having a lot of blank space and immature granulation tissue under the epithelium. The new skin in the HS group was longer and thicker. Further, the bFGF solution only and the bFGF-loaded HS groups exhibited regenerated extracellular matrix and a closed epidermal layer. After 14 days, in every group that received treatment, the wounds were entirely covered with new skin; however, a completely closed epidermal layer was not produced in the non-treated group. The bFGF-gel was the most effective among the four materials, and HS had a better performance than the control. The epidermal layers have a lot of capillaries and collagen deposition, and the skin histology features in the bFGF-HS group more resembled normal skin. Histological observations showed that wound healing by the HS loaded with bFGF was better than that of the other materials. Thus, our dressings have promising application prospects in wound healing.

The primary component of the extracellular matrix in the healing of wounds is collagen produced by fibroblasts [52–55]. To evaluate the quality of the regenerated skin, the number of hair follicles and collagen deposition were visualized by Masson's trichrome staining at 14 days after implantation. Collagen deposition in the blank HS group was mainly distributed in the upper epidermis near wound defect sites. However, collagen deposition in the bFGF-HS group was distributed in different parts of the epidermis and dermis, with evident deposition. Therefore, although collagen could be found in all four groups, bFGF gel treatment had the best wound healing effect based on the distribution and morphological observations of collagen (Fig. 4d). The bFGF-HS group's blue collagen composition was denser and thicker than that of the other three groups. Further, due of the synergistic effects of bFGF and HS, the maximum collagen deposition was seen in the bFGF-HS group. Only a few hair follicles were regenerated in the bFGF group because bFGF was quickly inactivated from the wound sites, whereas more hair follicles were seen in the regenerated tissues in the bFGF-HS group (Fig. 4e) owing to the retention of bFGF in HS. Therefore, HS are suitable for loading and releasing bFGF. Angiogenesis and inflammatory responses at the wound site were actively controlled by bFGF-HS, leading to quicker, scar-free skin regeneration and an increase in hair follicles. Therefore, the bFGF-HS promoted both wound remodeling to normal skin tissue and wound healing rate acceleration.

Human epidermal keratinocytes are essential for wound healing, and their proliferation and migration are connected to re-epithelialization. Patients with severe burns who lack epidermal keratinocytes would have longer disease duration, complications, and scar formation in the later stages [56,57]. We evaluated the effect of the bFGF-HS on wound healing by assessing keratinocyte proliferation. Keratinocytes exhibited a higher proliferation rate in wounds treated with the bFGF-HS than those treated with the HS

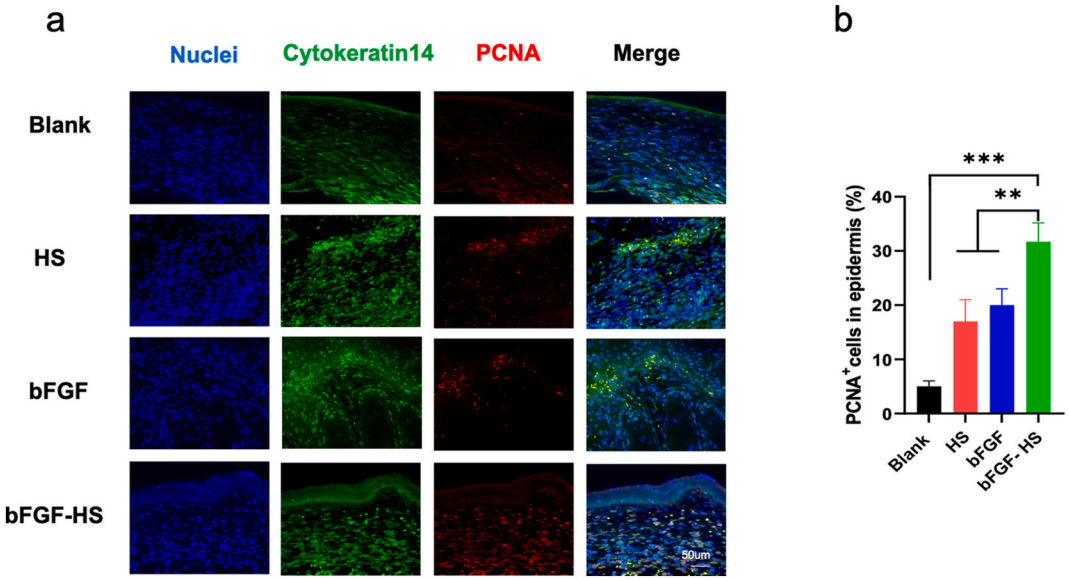

Fig. 5. The proliferation of keratinocytes (a) Cutaneous wounds on day 14 post-injury were stained with PCNA antibody (red), Cytokeratin 14 antibody (green), and DAPI antibody (blue) and micrographs were taken. Scale bar = 50 μm. (b) Quantification of the number of proliferating cell nuclear antigen (PCNA)-positive keratinocytes. Data are expressed as mean ± SD (n = 5). (For interpretation of the references to color in this figure legend, the reader is referred to the Web version of this article.)

gel and bFGF (Fig. 5a and b).

3.6. Macrophage infiltration

The inflammatory response is important for the wound healing process and quality [58]. M1 (pro-inflammatory state) is mainly expressed in the early stage of inflammation, which is responsible for promoting the inflammatory response by secreting pro-inflammatory factors. In the late stage, a key factor in the regeneration and healing of injured tissue is macrophage M1 (pro-inflammatory state)-M2 (anti-inflammatory state) switching. To control the granulation process and encourage cell proliferation, collagen deposition, and angiogenesis, M2 macrophages secrete a variety of anti-inflammatory factors as well as multiple GFs (VEGF and EGF). However, persistent inflammation may impede wound healing and leave behind scar tissue after healing [59–61].

In order to gauge the level of inflammation at the incision site, the CD68 antibody was used to label phagocytes. At 7 days after the operation, the amount of macrophages gradually decreased when the wounds were treated with HS, bFGF, and bFGF-HS (Fig. 6a and b). Further, comparing the bFGF-HS group to the other groups, the level of inflammation dramatically decreased. The highest ratio of M2/M1 macrophages (CD163/CD68) was observed in the bFGF-HS group, suggesting that macrophage polarization to M2 was increased at the wound sites following the introduction of bFGF-HS owing to the synergistic action of bFGF and HS(Fig. 6c). Overall, bFGF-HS can promote anastomosis healing with reduced scar formation.

3.7. Angiogenesis

As angiogenesis is a crucial element impacting the quality of wound healing [62], the formation of new blood vessels is indispensable for the survival, repair, and reshaping of wounded tissues. Neovascularization quantification can be used to assess the quality of wound healing. Smooth muscle actin (-SMA), a marker for angiogenesis, is expressed by mature myofibroblasts and smooth muscle cells in arterial walls. The level of angiogenesis may be determined by the expression of CD31, which is mostly found in the tight junctions between skin endothelial cells and is involved in blood vessel formantion. On day 14 post-implantation, To assess the neovascularization of wound tissue for the four groups and investigate the mode and extent of neovascularization under various treatments, IF staining with CD31 and -SMA antibodies was performed [63]. As shown in Fig. 7a–c, the number of blood vessels in the blank control group was the lowest. Further, the capillaries that formed during wound healing in the HS group were mostly circular and had a small diameter. In the bFGF and bFGF-HS groups, most newly formed capillaries were big, flat, and linear in shape. Furthermore, the bFGF-HS group had an increased capillary content than the other groups at 14 days After the procedure. These results indicate that the expression of SMA and CD31 in skin epidermal cells such keratinocytes and fibroblasts is influenced by bFGF-HS. And we proved that the angiogenesis-promoting properties of bFGF-HS were applicable to wound healing.

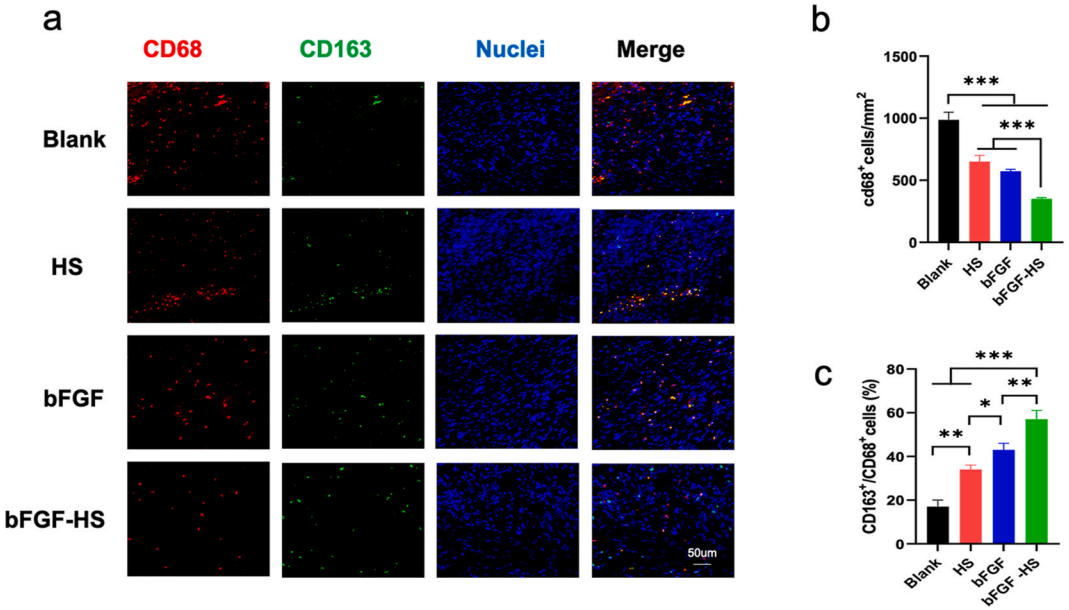

Fig. 6. Inflammation at wound sites in the different groups at 7 and 14 days post-surgery. (a) Immunofluorescent images of the tissue sections stained with the CD68 antibody (red) and DAPI (blue). Scale bars = 50 μm. (b) $CD68^+$ macrophage number per mm^2 at wound sites treated with the different materials. (c) The ratio of M2/M1 macrophages (CD163/CD68). Data are expressed as mean ± SD (n = 5). (For interpretation of the references to color in this figure legend, the reader is referred to the Web version of this article.)

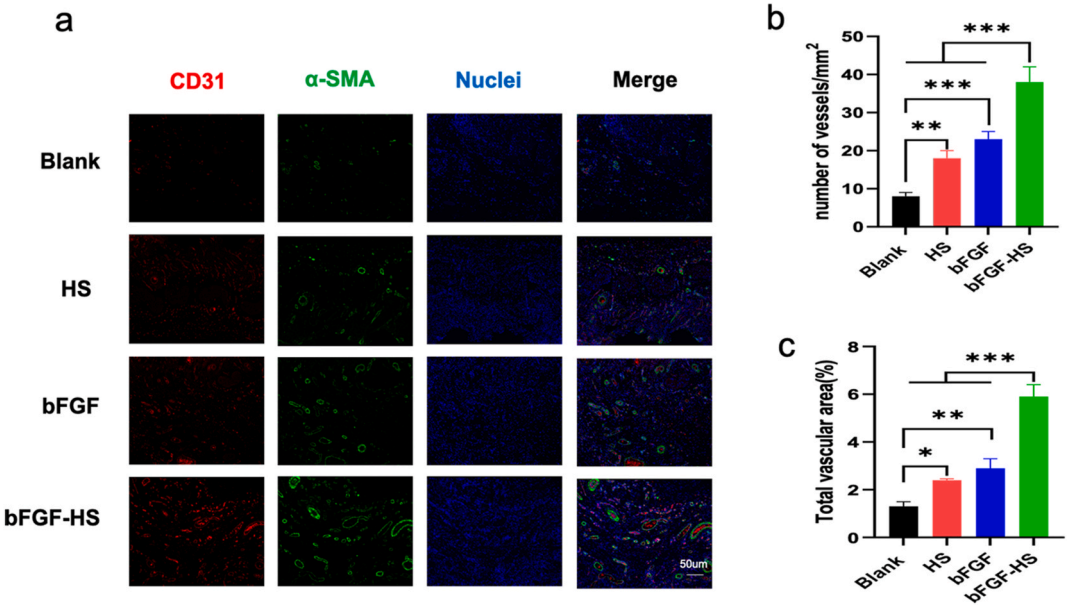

Fig. 7. Angiogenesis at wound sites in the different groups at 14 days post-surgery. (a) Immunofluorescent images of the tissue sections stained with the CD31 antibody (red), a-SMA antibody (green), and DAPI (blue). Scale bars = 50 mm. (b) Blood vessel numbers per mm^2 at wound sites treated with the different materials. (c) Percentage of CD31 vessel volume in the fluorescent images. Data are expressed as mean ± SD (n = 5). (For interpretation of the references to color in this figure legend, the reader is referred to the Web version of this article.)

4. Conclusions

In this study, biocompatible heparin-based sericin hydrogels prepared by the ultrasound cross-linking reaction of sericin were found to provide effective retention of loaded basic fibroblast growth factor . Heparin-based hydrogels exhibit rapid water uptake, swelling behavior, and suitable mechanical strength to serve as wound dressings. The experiments carried out using animals revealed that by speeding up wound healing, heparin-based sericin hydrogel-encapsulated bFGF is used to aid in wound closure, re-epithelialization, collagen synthesis, dermis formation, hair follicle formation, and angiogenesis over the entire wound-healing period.

Collectively, the results indicate that in therapeutic settings, heparin-based sericin hydrogel encapsulated bFGF dressing has the potential to accelerate wound healing.

However, burn wounds are also a medical problem that cannot be ignored. Our research lacks the exploration of burn wounds. Next, we will delve into the effect of our dressings on the healing of burn wounds to facilitate the next clinical application.

Abbreviations

Growth factors (GFs), Sericin hydrogel (S), basic fibroblast growth factor (bFGF), heparin-based sericin hydrogel (HS), sericin hydrogel -encapsulated basic fibroblast growth factor (bFGF-HS), three-dimensional (3D), Scanning electron microscope (SEM), swelling ratio (SR), degradation rate (DR), human dermal fibroblasts (HDFs), Human keratinocytes (HaCaT), Hematoxylin eosin (H&E), α-smooth muscle actin (α-SMA)

Declarations

Author contribution statement

Pan Du, Ling Diao, Guozhong Lv, Xue Chen: Conceived and designed the experiments; Performed the experiments; Analyzed and interpreted the data; Contributed reagents, materials, analysis tools or data.Yichi Lu: Performed the experiments; Analyzed and interpreted the data; Wrote the paper.Chenyang Liu, Jin Li, Yang Chen: Conceived and designed the experiments; Performed the experiments; Analyzed and interpreted the data; Contributed reagents, materials, analysis tools or data; Wrote the paper.Junfeng Chen: Conceived and designed the experiments; Contributed reagents, materials, analysis tools or data.

Funding statement

This work was supported by Stanford Center on the Demography and Economics of Health and Aging, Stanford University (2021ZHYB05).

Data availability statement

Data included in article/supp. Material/referenced in article.

Declaration of competing interest

The authors declare that they have no known competing financial interests or personal relationships that could have appeared to influence the work reported in this paper.

Acknowledgements

This work was supported by 2021 Wuxi Translational Medicine Center General Program (2021ZHYB05).

References

[1] H.S. Kim, X. Sun, J.H. Lee, H.W. Kim, X. Fu, K.W. Leong, Advanced drug delivery systems and artificial skin grafts for skin wound healing, Adv. Drug Deliv. Rev. 146 (2019) 209–239.
[2] L.M. Morton, T.J. Phillips, Wound healing and treating wounds: differential diagnosis and evaluation of chronic wounds, J. Am. Acad. Dermatol. 74 (4) (2016) 589–605, quiz 605-6.
[3] H. Nosrati, M. Khodaei, Z. Alizadeh, M. Banitalebi-Dehkordi, Cationic, anionic and neutral polysaccharides for skin tissue engineering and wound healing applications, Int. J. Biol. Macromol. 192 (2021) 298–322.
[4] L. Zhao, J. Zhao, F. Zhang, Z. Xu, F. Chen, Y. Shi, C. Hou, Y. Huang, C. Lin, R. Yu, W. Guo, Highly stretchable, adhesive, and self-healing silk fibroin-dopted hydrogels for wearable sensors, Adv Healthc Mater 10 (14) (2021), e2101062.
[5] S. El-Ashram, L.M. El-Samad, A.A. Basha, A. El Wakil, Naturally-derived targeted therapy for wound healing: beyond classical strategies, Pharmacol. Res. 170 (2021), 10574.
[6] R. Li, K. Liu, X. Huang, et al., Bioactive materials promote wound healing through modulation of cell behaviors, Adv. Sci. 9 (10) (2022), e2105152.
[7] M. Prasathkumar, S. Sadhasivam, Chitosan/Hyaluronic acid/Alginate and an assorted polymers loaded with honey, plant, and marine compounds for progressive wound healing-Know-how, Int. J. Biol. Macromol. 186 (2021) 656–685.
[8] B. Gorain, M. Pandey, N.H. Leng, C.W. Yan, K.W. Nie, S.J. Kaur, V. Marshall, S.P. Sisinthy, J. Panneerselvam, N. Molugulu, P. Kesharwani, H. Choudhury, Advanced drug delivery systems containing herbal components for wound healing, Int. J. Pharm. 617 (2022), 121617.
[9] S. Zhu, Y. Yu, Y. Ren, L. Xu, H. Wang, X. Ling, L. Jin, Y. Hu, H. Zhang, C. Miao, K. Guo, The emerging roles of neutrophil extracellular traps in wound healing, Cell Death Dis. 12 (11) (2021) 984.
[10] N. Amiri, A.P. Golin, R.B. Jalili, A. Ghahary, Roles of cutaneous cell-cell communication in wound healing outcome: an emphasis on keratinocyte-fibroblast crosstalk, Exp. Dermatol. 31 (4) (2022) 475–484.
[11] L.S. Ai, H.W. He, P. Wang, R. Cai, G. Tao, M.R. Yang, L.Y. Liu, H. Zuo, P. Zhao, Y.J. Wang, Rational design and fabrication of ZnONPs functionalized sericin/PVA antimicrobial sponge, Int. J. Mol. Sci. 20 (19) (2019).
[12] A. Kwiatkowska, M. Drabik, A. Lipko, A. Grzeczkowicz, R. Stachowiak, A. Marszalik, L.H. Granicka, Composite membrane dressings system with metallic nanoparticles as an antibacterial factor in wound healing, Membr. Biochem. 12 (2) (2022).
[13] G. Tao, R. Cai, Y.J. Wang, H. Zuo, H.W. He, Fabrication of antibacterial sericin based hydrogel as an injectable and mouldable wound dressing, Mat Sci Eng C-Mater 119 (2021).
[14] K. Banerjee, R. Madhyastha, Y. Nakajima, M. Maruyama, H. Madhyastha, Nanoceutical adjuvants as wound healing material: precepts and prospects, Int. J. Mol. Sci. 22 (9) (2021).
[15] J. Ahmed, M. Gultekinoglu, M. Edirisinghe, Bacterial cellulose micro-nano fibres for wound healing applications, Biotechnol. Adv. 41 (2020), 107549.
[16] W. Fang, L. Yang, L. Hong, Q. Hu, A chitosan hydrogel sealant with self-contractile characteristic: from rapid and long-term hemorrhage control to wound closure and repair, Carbohydr. Polym. 271 (2021), 118428.
[17] Y. Zhu, J. Zhang, J. Yang, C. Pan, T. Xu, L. Zhang, Zwitterionic hydrogels promote skin wound healing, J. Mater. Chem. B 4 (30) (2016) 5105–5111.
[18] J.R. Bardill, M.R. Laughter, M. Stager, K.W. Liechty, M.D. Krebs, C. Zgheib, Topical gel-based biomaterials for the treatment of diabetic foot ulcers, Acta Biomater. 138 (2022) 73–91.
[19] G. Tao, R. Cai, Y.J. Wang, L.Y. Liu, H. Zuo, P. Zhao, A. Umare, C.B. Mao, Q.Y. Xia, H.W. He, Bioinspired design of AgNPs embedded silk sericin-based sponges for efficiently combating bacteria and promoting wound healing, Mater. Des. 180 (2019).
[20] G. Tao, Y.J. Wang, R. Cai, H.P. Chang, K. Song, H. Zuo, P. Zhao, Q.Y. Xia, H.W. He, Design and performance of sericin/poly(vinyl alcohol) hydrogel as a drug delivery carrier for potential wound dressing application, Materials Science & Engineering C-Materials for Biological Applications 101 (2019) 341–351.
[21] B. Kundu, S.C. Kundu, Silk sericin/polyacrylamide in situ forming hydrogels for dermal reconstruction, Biomaterials 33 (30) (2012) 7456–7467.
[22] H. He, G. Tao, Y. Wang, R. Cai, P. Guo, L. Chen, H. Zuo, P. Zhao, Q. Xia, In situ green synthesis and characterization of sericin-silver nanoparticle composite with effective antibacterial activity and good biocompatibility, Mater Sci Eng C Mater Biol Appl 80 (2017) 509–516.
[23] P. Wang, H. He, R. Cai, G. Tao, M. Yang, H. Zuo, A. Umar, Y. Wang, Cross-linking of dialdehyde carboxymethyl cellulose with silk sericin to reinforce sericin film for potential biomedical application, Carbohydr. Polym. 212 (2019) 403–411.
[24] H. He, R. Cai, Y. Wang, G. Tao, P. Guo, H. Zuo, L. Chen, X. Liu, P. Zhao, Q. Xia, Preparation and characterization of silk sericin/PVA blend film with silver nanoparticles for potential antimicrobial application, Int. J. Biol. Macromol. 104 (Pt A) (2017) 457–464.
[25] Z.X. Huang, Y.J. Wang, M. Wu, W.T. Li, H. Zuo, B. Xiao, X.Q. Zhang, J. Wu, H.W. He, Q.Y. Xia, Sericin-based gadolinium nanoparticles as synergistically enhancing contrast agents for pH-responsive and tumor targeting magnetic resonance imaging, Mater. Des. 203 (2021).
[26] S. Baptista-Silva, S. Borges, A.R. Costa-Pinto, R. Costa, M. Amorim, J.R. Dias, O. Ramos, P. Alves, P.L. Granja, R. Soares, M. Pintado, A.L. Oliveira, In situ forming silk sericin-based hydrogel: a novel wound healing biomaterial, ACS Biomater. Sci. Eng. 7 (4) (2021) 1573–1586.
[27] J. Wu, J. Zhu, C. He, Z. Xiao, J. Ye, Y. Li, A. Chen, H. Zhang, X. Li, L. Lin, Y. Zhao, J. Zheng, J. Xiao, Comparative study of heparin-poloxamer hydrogel modified bFGF and aFGF for in vivo wound healing efficiency, ACS Appl. Mater. Interfaces 8 (29) (2016) 18710–18721.
[28] X. Chen, G. Tong, J. Fan, Y. Shen, N. Wang, W. Gong, Z. Hu, K. Zhu, X. Li, L. Jin, W. Cong, J. Xiao, Z. Zhu, FGF21 promotes migration and differentiation of epidermal cells during wound healing via SIRT1-dependent autophagy, Br. J. Pharmacol. 179 (5) (2022) 1102–1121.
[29] G. Shabestani Monfared, P. Ertl, M. Rothbauer, An on-chip wound healing assay fabricated by xurography for evaluation of dermal fibroblast cell migration and wound closure, Sci. Rep. 10 (1) (2020), 16192.
[30] M. Bahadoran, A. Shamloo, Y.D. Nokoorani, Development of a polyvinyl alcohol/sodium alginate hydrogel-based scaffold incorporating bFGF-encapsulated microspheres for accelerated wound healing, Sci. Rep. 10 (1) (2020) 7342.
[31] X. Xuan, Y. Zhou, A. Chen, S. Zheng, Y. An, H. He, W. Huang, Y. Chen, Y. Yang, S. Li, T. Xuan, J. Xiao, X. Li, J. Wu, Silver crosslinked injectable bFGF-eluting supramolecular hydrogels speed up infected wound healing, J. Mater. Chem. B 8 (7) (2020) 1359–1370.
[32] J. Wu, J. Zhu, C. He, Z. Xiao, J. Ye, Y. Li, A. Chen, H. Zhang, X. Li, L. Lin, Y. Zhao, J. Zheng, J. Xiao, Comparative study of heparin-poloxamer hydrogel modified bFGF and aFGF for in vivo wound healing efficiency, ACS Appl. Mater. Interfaces 8 (29) (2016) 18710–18721.

[33] A. Zieris, K. Chwalek, S. Prokoph, K.R. Levental, P.B. Welzel, U. Freudenberg, C. Werner, Dual independent delivery of pro-angiogenic growth factors from starPEG-heparin hydrogels, J. Contr. Release 156 (1) (2011) 28–36.
[34] A. Yayon, M. Klagsbrun, J.D. Esko, P. Leder, D.M. Ornitz, Cell surface, heparin-like molecules are required for binding of basic fibroblast growth factor to its high affinity receptor, Cell 64 (4) (1991) 841–848.
[35] S. Faham, R.E. Hileman, J.R. Fromm, R.J. Linhardt, D.C. Rees, Heparin structure and interactions with basic fibroblast growth factor, Science 271 (5252) (1996) 1116–1120.
[36] X. Shen, Z. Liu, J. Li, D. Wu, M. Zhu, L. Yan, G. Mao, X. Ye, R.J. Linhardt, S. Chen, Development of low molecular weight heparin by H2O2/ascorbic acid with ultrasonic power and its anti-metastasis property, Int. J. Biol. Macromol. 133 (2019) 101–109.
[37] H.L. Xu, F.R. Tian, J. Xiao, P.P. Chen, J. Xu, Z.L. Fan, J.J. Yang, C.T. Lu, Y.Z. Zhao, Sustained-release of FGF-2 from a hybrid hydrogel of heparin-poloxamer and decellular matrix promotes the neuroprotective effects of proteins after spinal injury, Int. J. Nanomed. 13 (2018) 681–694.
[38] J. Wu, J. Zhu, C. He, Z. Xiao, J. Ye, Y. Li, A. Chen, H. Zhang, X. Li, L. Lin, Y. Zhao, J. Zheng, J. Xiao, Comparative study of heparin-poloxamer hydrogel modified bFGF and aFGF for in vivo wound healing efficiency, ACS Appl. Mater. Interfaces 8 (29) (2016) 18710–18721.
[39] H.T. Hsieh, H.M. Chang, W.J. Lin, Y.T. Hsu, F.D. Mai, Poly-methyl methacrylate/polyvinyl alcohol copolymer agents applied on diabetic wound dressing, Sci. Rep. 7 (1) (2017) 9531.
[40] J.D. Li, Z.Z. Ding, X. Zheng, G.Z. Lu, Q. Lu, D.L. Kaplan, Injectable silk nanofiber hydrogels as stem cell carriers to accelerate wound healing, J. Mater. Chem. B 9 (37) (2021) 7771–7781.
[41] H. Matsumoto, Y. Kumon, H. Watanabe, T. Ohnishi, M. Shudou, C. Ii, H. Takahashi, Y. Imai, J. Tanaka, Antibodies to CD11b, CD68, and lectin label neutrophils rather than microglia in traumatic and ischemic brain lesions, J. Neurosci. Res. 85 (5) (2007) 994–1009.
[42] X.M. Dai, Q.Q. Guo, Y. Zhao, P. Zhang, T.Q. Zhang, X.G. Zhang, C.X. Li, Functional silver nanoparticle as a benign antimicrobial agent that eradicates antibiotic-resistant bacteria and promotes wound healing, Acs Appl Mater Inter 8 (39) (2016) 25798–25807.
[43] Z. Wang, W. Hu, Y. Du, Y. Xiao, X. Wang, S. Zhang, J. Wang, C. Mao, Green gas-mediated cross-linking generates biomolecular hydrogels with enhanced strength and excellent hemostasis for wound healing, ACS Appl. Mater. Interfaces 12 (12) (2020) 13622–13633.
[44] T. Li, H.S. Ma, H.Z. Ma, Z.J. Ma, L. Qiang, Z.Z. Yang, X.X. Yang, X.J. Zhou, K.R. Dai, J.W. Wang, Mussel-inspired nanostructures potentiate the immunomodulatory properties and angiogenesis of mesenchymal stem cells, Acs Appl Mater Inter 11 (19) (2019) 17134–17146.
[45] M. Zhu, Y. Chu, Q. Shang, et al., Mesenchymal stromal cells pretreated with pro-inflammatory cytokines promote skin wound healing through VEGFC-mediated angiogenesis, Stem Cells Transl Med 9 (10) (2020) 1218–1232.
[46] N. Stephanopoulos, J.H. Ortony, S.I. Stupp, Self-assembly for the synthesis of functional biomaterials, Acta Mater. 61 (3) (2013) 912–930.
[47] X. Wang, J.A. Kluge, G.G. Leisk, D.L. Kaplan, Sonication-induced gelation of silk fibroin for cell encapsulation, Biomaterials 29 (8) (2008) 1054–1064.
[48] T. Vu, Y. Xue, T. Vuong, M. Erbe, C. Bennet, B. Palazzo, L. Popielski, N. Rodriguez, X. Hu, Comparative study of ultrasonication-induced and naturally self-assembled silk fibroin-wool keratin hydrogel biomaterials, Int. J. Mol. Sci. 17 (9) (2016).
[49] G. Gabbiani, G.B. Ryan, G. Majne, Presence of modified fibroblasts in granulation tissue and their possible role in wound contraction, Experientia 27 (5) (1971) 49–550.
[50] R.F. Diegelmann, M.C. Evans, Wound healing: an overview of acute, fibrotic and delayed healing, Front. Biosci. 9 (2004) 283–289.
[51] J.C. Lai, H.Y. Lai, K.R. Nalamolu, S.F. Ng, Treatment for diabetic ulcer wounds using a fern tannin optimized hydrogel formulation with antibacterial and antioxidative properties, J. Ethnopharmacol. 89 (2016) 77–289.
[52] Y. Garcia, N. Hemantkumar, R. Collighan, M. Griffin, J.C. Rodriguez-Cabello, A. Pandit, In vitro characterization of a collagen scaffold enzymatically cross-linked with a tailored elastin-like polymer, Tissue Eng. 15 (4) (2009) 887–899.
[53] P. Monika, P.V. Waiker, M.N. Chandraprabha, A. Rangarajan, K.N.C. Murthy, Myofibroblast progeny in wound biology and wound healing studies, Wound Repair Regen. 29 (4) (2021) 531–547.
[54] M. Budhiraja, S. Zafar, S. Akhter, M. Alrobaian, M.A. Rashid, M.A. Barkat, S. Beg, F.J. Ahmad, Mupirocin-loaded chitosan microspheres embedded in piper betle extract containing collagen scaffold accelerate wound healing activity, AAPS PharmSciTech 23 (3) (2022).
[55] L.H.H. Cheng, X.X. Lei, Z.J. Yang, Y.A. Kong, P.C. Xu, S.Y. Peng, J. Wang, C. Chen, Y.Q. Dong, X.H. Hu, X.R. Zhang, T. Forouzanfar, G. Wu, X.B. Fu, Histatin 1 enhanced the speed and quality of wound healing through regulating the behaviour of fibroblast, Cell Prolif 54 (8) (2021).
[56] X.X. Li, C.W. Liu, Y.W. Zhu, H.Y. Rao, M. Liu, L.M. Gui, W.X. Feng, H.Y. Tang, J. Xu, W.Q. Gao, L. Li, SETD2 epidermal deficiency promotes cutaneous wound healing via activation of AKT/mTOR Signalling, Cell Prolif 54 (6) (2021).
[57] V. Falanga, Wound healing and its impairment in the diabetic foot, Lancet 366 (9498) (2005) 1736–1743.
[58] J.Q. Coentro, E. Pugliese, G. Hanley, M. Raghunath, D.I. Zeugolis, Current and upcoming therapies to modulate skin scarring and fibrosis, Adv. Drug Deliv. Rev. 146 (2019) 37–59.
[59] A.E. Louiselle, S.M. Niemiec, C. Zgheib, K.W. Liechty, Macrophage polarization and diabetic wound healing, Transl. Res. 236 (2021) 109–116.
[60] H. Kim, S.Y. Wang, G. Kwak, Y. Yang, I.C. Kwon, S.H. Kim, Exosome-guided phenotypic switch of M1 to M2 macrophages for cutaneous wound healing, Adv. Sci. 6 (20) (2019).
[61] S.W. Kim, G.B. Im, G.J. Jeong, S. Baik, J. Hyun, Y.J. Kim, C. Pang, Y.C. Jang, S.H. Bhang, Delivery of a spheroids-incorporated human dermal fibroblast sheet increases angiogenesis and M2 polarization for wound healing, Biomaterials 275 (2021).
[62] A.P. Veith, K. Henderson, A. Spencer, A.D.O.B.E. Univer, A.B. Baker, Therapeutic strategies for enhancing angiogenesis in wound healing, Adv. Drug Deliv. Rev. 146 (2019) 97–125.
[63] C.Y. Wang, C.Y. Liang, R. Wang, X.L. Yao, P. Guo, W.Z. Yuan, Y. Liu, Y. Song, Z.H. Li, X.Y. Xie, The fabrication of a highly efficient self-healing hydrogel from natural biopolymers loaded with exosomes for the synergistic promotion of severe wound healing, Biomater Sci-Uk 8 (1) (2020) 313–324.